Popa, C.O. and Haragâş, S., 2017. Some considerations regarding the fatigue cracks producing pitting wear of gears. *Romanian Journal of Technical Sciences – Applied Mechanics, 62(2)*, pp.163–179.

SOME CONSIDERATIONS REGARDING THE FATIGUE CRACKS PRODUCING PITTING WEAR OF GEARS

CLAUDIU OVIDIU POPA, SIMION HARAGÂŞ

Abstract. In this article some aspects of the fatigue cracks that have the consequence of pitting wear appearance on the spur gears are presented. The main mechanisms leading to the fatigue cracks, crack nucleation, propagation of cracks of small length, as well as the propagation of cracks on long lengths, respectively, will also be analyzed. The stress field, the growth rate as well as the spread of fatigue cracks will be considered.

Key words: fatigue crack, gear, crack nucleation, small length cracks, stresses field, fatigue cracks propagation.

1. INTRODUCTION

Pitting wear is the main cause of gears tooth flank destruction, made of materials with low and medium hardness (HB < 3500 MPa). Thus, after a running time ($N > 10^4$ cycles), some pits appear on the surface of the teeth.

The first signs of fatigue usually appear in the area of rolling gears in the form of micro-cracks. Initially, these micro-cracks appear in the sense of the friction forces, which on the drive gear are from the pitch circle to the foot circle and head circles and reverse to the driven gear, due to the fact that the relative speed between the two flanks changes their sense in the pitch point.

The oil, which adheres to the tooth surface, is pressed – by the flank of the conjugated tooth – into the existing micro-cracks. A hydrostatic pressure occurs in the crack area, which favours the growth of the micro-cracks and the decomposition of small pieces of material, resulting in the appearance of small pits on the active surfaces of the teeth.

Initial pitting is usually caused by gear-tooth surfaces not properly conforming to each other, or not fitting together properly. This can be a result of minor involute errors or local surface irregularities, but most often it occurs because is not proper alignment across the full face width of the gear mesh.

Corresponding to the destructive pitting, the surface pits are usually considerably larger in diameter than those associated with initial pitting.

Technical University of Cluj-Napoca, Romania

The dedendum section of the drive gear is often the first to experience serious pitting damage; however, as operation continues, pitting usually progresses to the point where a considerable area of the tooth surfaces have developed pitting craters of various shapes and sizes.

Destructive pitting usually results from surface overload which cannot be alleviated by corrective (initial) pitting. Once enough stress cycles have been built up, pitting continues until the tooth profile is completely destroyed, causing extremely rough operation and considerable noise.

Often a bending fatigue crack will originate from a pit, causing premature tooth breakage failure.

As has been shown, the appearance of pitting is due to the existence of a fatigue crack that increases over time.

This requires an analysis of how these cracks originate, as well as the mechanisms underlying their propagation.

2. FATIGUE CRACK INITIATION

2.1. Crack initiation stages

Generally viewed, current methods of predicting fatigue life in metallic components take into account 3 stages (Fig. 1):

1. Initiation of the fatigue crack;

2. The development of a crack in the macroscopic crack, or other formations (e.g., rounded holes or cavities), propagation or coalescence;

3. Long-range propagation, over a certain critical value, resulting in the destruction of the piece through fatigue.

The last two stages can be studied using Linear Elastic Fracture Mechanics (LEFM) or Elasto-Plastic Fracture Mechanics (EPFM).

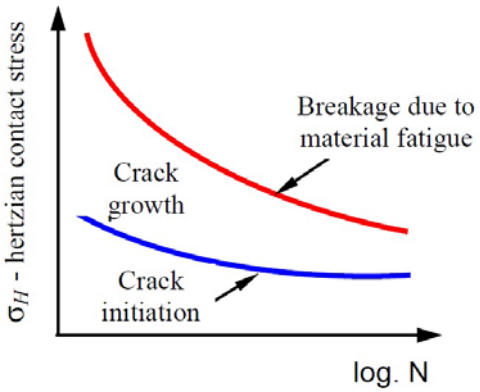

Fig. 1 – The stages of fatigue life.

The crack initiation stage can be divided into two stages:

1. The nucleation of the crack, by mechanisms determined by the static and dynamic equilibrium of the dislocations;

2. The extension of the nucleation process, respectively the increase over a small length of the crack.

Nucleation of the micro-crack implies the appearance of the first sliding bands in crystalline grains. A sliding band is the range in which there are a large number of marginal dislocations with the possibility of movement. The presence of an obstacle in the movement plane of dislocations, such as grain boundaries, inclusion of hard particles, leads to an agglomeration of obstacle dislocations and has the effect of inducing a strong tension concentration on the obstacle boundary.

The Fig. 2 presents a section through a material which shows the existence of structural inclusions, of a structure, different from that of the base matrix. [6]

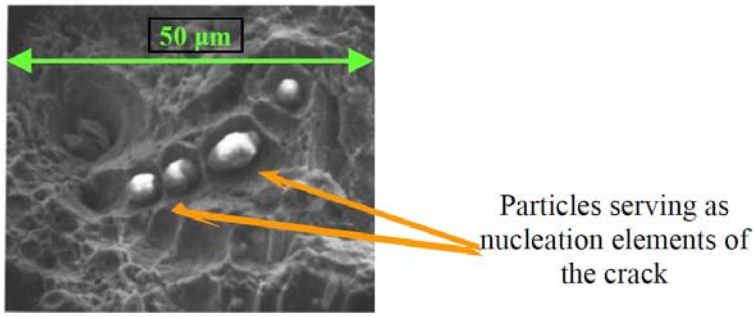

Fig. 2 – Particles serving as nucleation elements of the crack.

2.2. Fatigue crack nucleation model

There is only a limited number of models that aim to analyze the crack nucleation stage, i.e. the growth of crack in small length, most of the models relying on dislocation theory to explain the accumulation of damage in the microstructure of the material.

In the following, the Tanaka-Mura model [20, 23, 27] is briefly presented. This model is applied to metallic components in which the nucleation process occurs by fracture given by trans-granular tangential stresses and it assumes that the crack nucleates when the critical strain energy is exceeded.

If a load, greater than the local stress of a grain of diameter d_{gr} is applied, generated displacements are moving along a sliding plane of a length w_T (Fig. 3). Dislocations accumulate at the grain boundary, which constitutes a barrier to their movement.

The displacement is considered to be irreversible, so that when reversing the load, the dislocations will accumulate in the free plane in the vicinity of them.

Because the residual load given by the reverse stress generated by the positive displacements acts in the same direction as the inverse load, the displacement of the negative displacements occurs during the period when there is no load.

Along each stress cycle, the number of dislocations increases monotonously.

For the first load, the equilibrium condition is [27]:

$$\tau_{inv}^{D} + \left(\tau_{1d} - \tau_{fd}\right) = 0\,, \tag{1}$$

where τ_{fd} there is the frictional tension and had the physical significance of the material's resistance to the movement of the dislocation. This tension is a function of Rockwell's hardness of material, temperature and material flow.

In order to move the dislocation, the tangential tension τ_{1d} due to all dislocations in the sliding band at the first load must exceed the value τ_{fd}; with τ_{inv}^{D} the reverse tangential stress (reaction) due to the movement of the dislocations was noted.

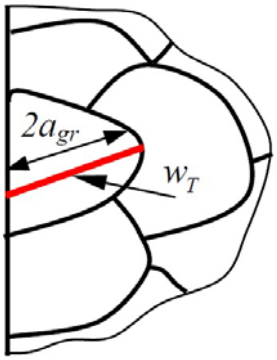

Fig. 3 – Sliding bands interacting with grain boundary.

If the density of the dislocations $D_1(\xi)$ along the sliding plane (in one direction) is continuous, then [27]:

$$\tau_{inv}^{D} = A_d \cdot \int_{-a_{gr}}^{a_{gr}} \frac{D_1(\xi')}{\xi - \xi'} \mathrm{d}\xi', \tag{2}$$

where:

$$A_d = \begin{cases} \dfrac{G}{2\pi(1-\nu)} & \text{for marginal dislocations} \\ \dfrac{G}{2\pi} & \text{for elicoidal dislocations} \end{cases} \tag{3}$$

where a_{gr} is the radius of the grain, G is the modulus of the transverse elasticity, and ν is the Poisson coefficient.

Using the Muskhelishvili [17] relationship for the endless density of dislocations at the grain boundary, it can be written [27]:

$$D_1(\xi) = \frac{\left(\tau_{1d} - \tau_{fd}\right) \cdot \xi}{\pi A_d \cdot \sqrt{a_{gr}^2 - \xi^2}}. \tag{4}$$

The incremental increase in dislocation density $\Delta D_1(\xi)$, with each cycle, is [27]:

$$\Delta D_1(\xi) = \frac{\left(\Delta\tau_{1d} - 2\tau_{fd}\right) \cdot \xi}{\pi A_d \cdot \sqrt{a_{gr}^2 - \xi^2}}. \tag{5}$$

The sliding displacement corresponding to the increment $\Delta D(\xi)$ is [27]:

$$\Phi_T(\xi) = \int_x^{a_{gr}} \Delta D(\xi) d\xi. \tag{6}$$

The increment of plastic deformation $\Delta\gamma_d$ is [27]:

$$\Delta\gamma_d = \int_{-a_{gr}}^{a_{gr}} \Phi_T(\xi) d\xi = \frac{\left(\Delta\tau_d - 2\tau_{fd}\right) \cdot a_{gr}^2}{2A_d}. \tag{7}$$

so, the equation describing the stress-strain hysteresis loop (Fig. 4) is [27]:

$$\gamma_d = \frac{\left(\tau_d - \tau_{fd}\right) \cdot a_{gr}^2}{2A_d}. \tag{8}$$

During the first load with the tension τ_{1d}, the material is hardened for any tensions that exceed τ_{fd} (Fig. 4). Upon reversing the load till τ_{2d}, the ABC curve is followed. At the next load, the CDA trace is followed.

The dimension of the plastic strain increment is a linear function of $(\tau_d - \tau_{fd})$. The dislocation deformation energy is the same for both direct and reverse load, except for the first load.

The deformation energy of the stored dislocations corresponds to the colored area of Fig. 4 and is determined by the relation [27]:

$$\Delta U_d = \Delta\gamma_d \cdot \left(\Delta\tau_d - 2\tau_{fd}\right). \tag{9}$$

The energy associated with the uncolored area (Fig. 4) is the work dissipated to overcome the frictional tension.

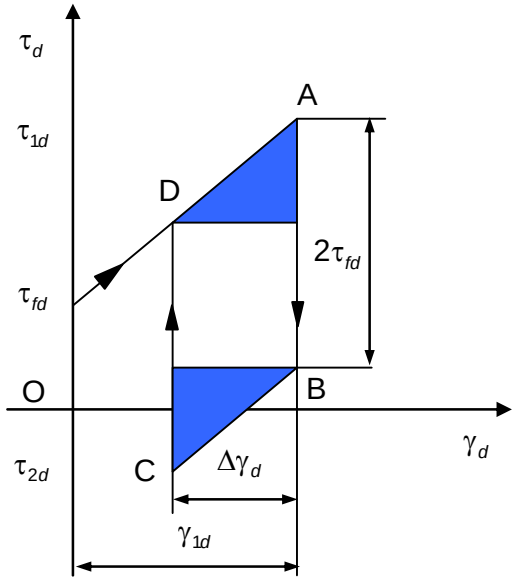

Fig. 4 – The stress-strain hysteresis loop.

Crack nucleation occurs when the total energy stored after N_n cycles is equal to the grain breaking energy [27]:

$$N_n \cdot \Delta U_d = 2a_{gr} W_s \tag{10}$$

$$N_n = \frac{4GW_s}{\left(\Delta\tau_d - 2\tau_{fd}\right)^2 \pi(1-\nu)\cdot d_{gr}}, \tag{11}$$

where d_{gr} is the diameter of the grain and W_s is the breaking energy specific to the surface unit of the grain. Equation (11) can also be written as [23, 27]:

$$\Delta\tau_d = 2\tau_{fd} + \left[\frac{4GW_S}{\pi(1-\nu)}\right]^{\frac{1}{2}} d_{gr}^{-1/2}, \tag{12}$$

which is the form of the Hall-Petch equation for the dependence between fatigue strength and grain size [27].

The proposed model has several approximations and limitations such as:

– the grains are homogeneous, not isotropic (dislocations can move freely to grain boundaries);

– the defects accumulate in a single planar sliding system. Generally, grains in a polycrystalline aggregate do not deform, but are constrained by neighboring grains. Nucleation of the crack occurs on the surface of the grains that are not as constrained as the embedded ones inside the material;

– the size of the nucleation of the crack is equal to the size of the grain;

– movement of dislocations is irreversible; However, it is likely that some dislocations will move back inside the grain, under the reverse load, but the experimental results show that they are just few;

– the number of saturation cycles is negligible.

The model shows that fatigue life is inversely proportional to the square of the amplitude of the plastic deformation, corresponding to the Coffin-Manson empirical equation.

Table 1 shows the average values of some parameters used in modeling.

Table 1

The average values of some parameters used in the above model

The variable	Value	M.U.	Description
d_{gr}	55.8	μm	Average grain diameter
G	$76 \cdot 10^3$	MPa	The transverse elastic modulus of the material
k_{fd}	69	MPa	The friction forces tension
ν	0.3	–	Poisson's coefficient
W_s	440	kN/m	The specific breaking energy of the grain

3. THE GROWTH OF THE CRACKS OF SMALL LENGTH

A small crack can be considered a crack having the size of a microstructure, whose propagation consists of a continuous re-opening of the crack in the sliding bands through transverse slides caused by the movement of the dislocations.

Their behavior differs from that of the long cracks; among the factors responsible for this can be remembered:

– a high rate of growth due to the lack of obstacles at the surface of the piece, but also due to the plane tensions in that area;

– a slowing of the crack growth due to microstructural obstacles.

Plasticity tends to focus along the sliding planes, causing the crack to rise along them. The sliding plan is not necessarily perpendicular to the applied stress field, which causes the crack to grow in different modes. Thus, when the crack is small, it can grow more easily along preferential planes. Large cracks need to grow simultaneously in several grains [5, 7, 19].

The models developed by the researchers to reproduce the behavior of small fatigue cracks [1, 3, 13, 19, 24] have been oriented in two directions, namely: one of the directions aimed at determining the stress intensity factors taking into account the microstructural heterogeneities (a long-crack-like propagation method) and another was the one that tries to explain the increase of the crack using the dislocation theory.

In Fig. 5, various cracks, ranging from intra-granular ones, to the cracks of the size of several grains are observed [15].

Chan [3] introduced the concept of "microstructural difference" which takes into account that the small cracks are actually in only a few grains. In this case, the average properties of the material at the tip of the crack vary significantly with respect to the mass of the material. Using an equivalent property model, it reduced the small crack growth to a one-dimensional problem.

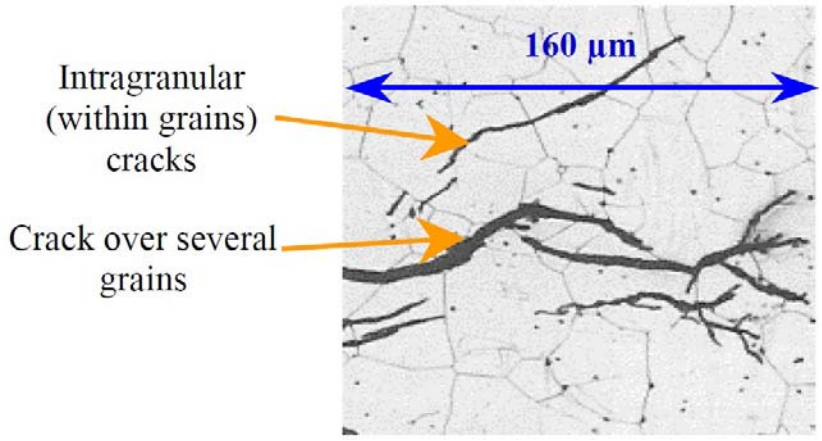

Fig. 5 – Different small and long cracks in steel [15].

Bilby [1] described the destruction near the crack tip by proposing a growth law based on the stress intensity factor for small cracks.

Tanaka [24] used a Monte Carlo simulation to predict the general behavior of small cracks. The random variables considered include the grain size, the frictional stresses between the grains, and the fact that one of the grains on the surface is loaded, ultimately achieving a similar growth trend to that found experimentally.

4. THE FATIGUE CRACKS PROPAGATION

Once the crack has initiate either in the substrate or at the surface of the gear tooth, if variable stresses continue, it will develop over a length sufficiently large to cause the piece to break (for example at the base of the tooth) or to change its working parameters, and the functioning still becoming inappropriate.

In the study of the fatigue crack propagation, the most important aspects are related to the determination of the stress fields in the vicinity of the crack, depending on the general state of loading of the piece, the angle at which the crack develops and its growth rate.

4.1. The stresses field near the crack tip. Stress intensity factor

A $2a$ length crack positioned in a plate subject to infinite stretching and a polar coordinate point $z_{a1} = r_{a1}e^{i\theta_{a1}}$ is considered (Fig. 6).

If the point M is very close to the crack tip ($r_a << a$)), then the stresses acting on the elemental surface are [2, 3, 9]:

$$\sigma_x = \sigma\sqrt{\frac{a}{2r_a}}\cdot\cos\frac{\theta_a}{2}\cdot\left(1-\sin\frac{\theta_a}{2}\cdot\sin\frac{3\theta_a}{2}\right) \tag{13}$$

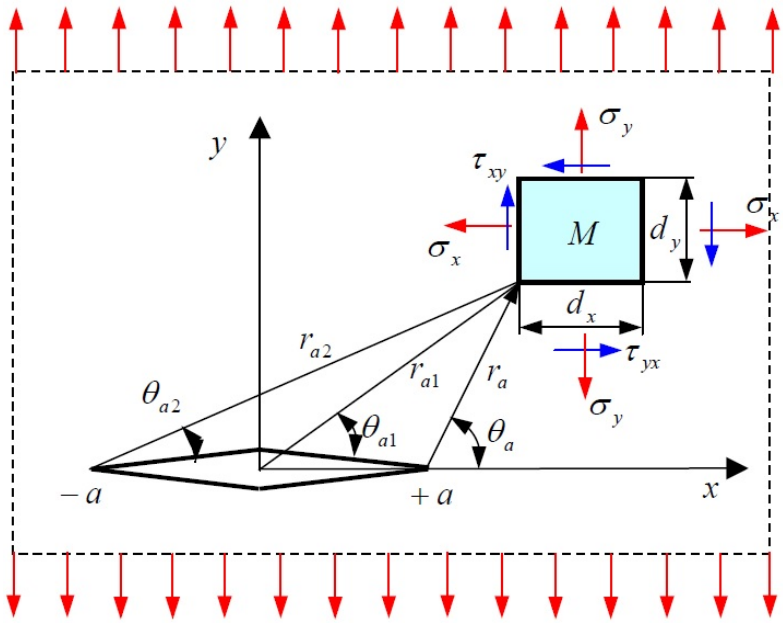

Fig. 6 – Crack in a plate subject to infinite stretching.

$$\sigma_y = \sigma\sqrt{\frac{a}{2r_a}}\cdot\cos\frac{\theta_a}{2}\cdot\left(1+\sin\frac{\theta_a}{2}\cdot\sin\frac{3\theta_a}{2}\right) \tag{14}$$

$$\tau_{xy} = \frac{\sigma}{2}\cdot\sqrt{\frac{a}{2r_a}}\cdot\sin\theta_a\cdot\cos\frac{3\theta_a}{2} \tag{15}$$

It is noted that in the relations above, the stress field at the point considered in the vicinity of the crack tip, although having a singular character, is expressed as the product of a factor:

$$k_a = \sigma \cdot \sqrt{a}\ , \tag{16}$$

which incorporates the stress intensity and the crack size, a single factor $1/\sqrt{2r_a}$ and three angular functions $f_x(\theta_a)$, $f_y(\theta_a)$ and $f_{xy}(\theta_a)$.

With this, it can be written [2, 4]:

$$\sigma_x = \frac{k_a}{\sqrt{2r_a}} \cdot f_x(\theta_a) = \frac{k}{\sqrt{2r_a}} \cdot \cos\frac{\theta_a}{2} \cdot \left(1 - \sin\frac{\theta_a}{2} \cdot \sin\frac{3\theta_a}{2}\right) \tag{17}$$

$$\sigma_y = \frac{k_a}{\sqrt{2r_a}} \cdot f_y(\theta_a) = \frac{k_a}{\sqrt{2r_a}} \cdot \cos\frac{\theta_a}{2} \cdot \left(1 + \sin\frac{\theta_a}{2} \cdot \sin\frac{3\theta_a}{2}\right) \tag{18}$$

$$\tau_{xy} = \frac{k_a}{\sqrt{2r_a}} \cdot f_{xy}(\theta_a) = \frac{k_a}{\sqrt{2r_a}} \cdot \cos\frac{\theta_a}{2} \cdot \sin\frac{\theta_a}{2} \cdot \cos\frac{3\theta_a}{2}\ . \tag{19}$$

It is usual to note the main part of singularity through a measure proportional to k_a, named [2, 3, 16]

$$K = \sqrt{\pi \cdot k_a} = \sigma \cdot \sqrt{\pi a} \quad [\text{MPa}\sqrt{\text{mm}}\ ], \tag{20}$$

stress intensity factor (SIF).

According to Irwin [9], in the most general case, the edges of a crack can have three independent kinematic movements, named fundamental modes of materials fracture.

The three fundamental fracture modes are differentiated as follows:

– Mode I, or traction mode; in the case of cracks, the normal displacement vector on the crack plane causes the crack to open; to this mode it corresponds SIF K_I;

– Mode II, or sliding mode; the displacement vector contained in the crack plane, normally on the front of the crack produces flat sliding: SIF is noted K_{II};

– Mode III, or anti-plane slip; the displacement vector comprised in the crack plane, parallel to the crack front, produces the anti-plane slip; it corresponds to K_{III}

The components of the stress state in the most general load case have a singularity proportional to $1/\sqrt{2\pi r_a}$ for all modes of displacement, so that the stress intensity factors can be separated and also the angle functions $f_{Ix}(\theta_a)$, $f_{Iy}(\theta_a)$, $f_{Ixy}(\theta_a)$, $f_{IIx}(\theta_a)$, ..., $f_{IIIx}(\theta_a)$ associated with each mode.

Thus, the general expressions of the stress state components are [4, 8, 10, 14]:

$$\sigma_x = \frac{1}{\sqrt{2\pi r_a}} \cdot \left[K_I \cdot f_{Ix}(\theta_a) + K_{II} \cdot f_{IIx}(\theta_a) + K_{III} \cdot f_{IIIx}(\theta_a)\right] \tag{21}$$

$$\sigma_y = \frac{1}{\sqrt{2\pi r_a}} \cdot \left[K_I \cdot f_{Iy}(\theta_a) + K_{II} \cdot f_{IIy}(\theta_a) + K_{III} \cdot f_{IIIy}(\theta_a) \right] \tag{22}$$

$$\tau_{xy} = \frac{1}{\sqrt{2\pi r_a}} \cdot \left[K_I \cdot f_{Ixy}(\theta_a) + K_{II} \cdot f_{IIxy}(\theta_a) + K_{III} \cdot f_{IIIxy}(\theta_a) \right]. \tag{23}$$

In polar coordinates, the equations defining the stress field at the crack tip are [10]:

$$\sigma_\theta = \frac{1}{\sqrt{2\pi r_a}} \left\{ \left[\frac{K_I}{2} \cdot \cos\frac{\theta_a}{2} \cdot (1 + \cos\theta_a) \right] - \left[3\frac{K_{II}}{2} \cdot \sin\frac{\theta_a}{2} \cdot (1 + \cos\theta_a) \right] \right\} \tag{24}$$

$$\sigma_r = \frac{1}{\sqrt{2\pi r_a}} \left\{ \left[\frac{K_I}{2} \cdot \cos\frac{\theta_a}{2} \cdot (3 - \cos\theta_a) \right] - \left[\frac{K_{II}}{2} \cdot \sin\frac{\theta_a}{2} \cdot (1 - 3\cos\theta_a) \right] \right\} \tag{25}$$

$$\tau_{r\theta} = \frac{1}{\sqrt{2\pi r_a}} \cdot \left\{ \left[\frac{K_I}{2} \cdot \sin\frac{\theta_a}{2} \cdot (1 + \cos\theta_a) \right] - \left[\frac{K_{II}}{2} \cdot \cos\frac{\theta_a}{2} \cdot (1 - 3\cos\theta_a) \right] \right\}. \tag{26}$$

The actual expressions of the tension intensity factors (SIF) K_I, K_{II} and K_{III} depend on the geometry of the body, on the actual mode of distribution of forces and moments and are presented in the specialty literature.

All of these elements are the basis for establishing the stresses field on the surface or in the substrate of the spur gear teeth, aspects that will be presented in another paper.

4.2. Fatigue crack growth rate

The modeling of crack propagation by variable stresses requires the explanation of the essential mechanisms that generate the propagation of the cracks and their inclusion in quantitative relations, from which the explicit relations of the propagation rate are obtained according to the parameters included in the model.

Generally, both in the case of empirical interpretations and also in the case of models correlating the phenomenon of the propagation of the crack with the fundamental processes of resistance of the material at the tip of the crack, relations of form [4, 12] are obtained:

$$\mathrm{d}a/\mathrm{d}N = f\left(a, \sigma_i, L_j, C_k\right), \tag{27}$$

in which $\mathrm{d}a/\mathrm{d}N$ is the crack propagation rate, σ_i describes the intensity of the stress, L_j comprises parameters of the nature of linear dimensions that describe the body geometry and C_k represent parameters and constants which describe the mechanical and other physical characteristics associated with the material.

The experimental observations show that in case of strong tension concentrators, up to 95% of the durability of the gear is consumed in the propagation of the dominant crack that ultimately leads to pitting.

Various analytical forms of the relationship (27) are known in the literature.

Paris [18], considering that the stress intensity factor univocally defines the field of stresses and deformations in the area adjacent to the crack tip, even if a limited plastic area is formed, suggested the idea of correlating this parameter with the crack propagation speed of the crack, through a relation of form (28), i.e.:

$$\mathrm{d}a/\mathrm{d}N = C_p\left(\Delta K\right)^{n_p}, \tag{28}$$

in which ΔK, according to the relation (29), is the variation of the stress intensity factor corresponding to the maximum values of $\sigma_{\max}$ and minimum values $\sigma_{\min}$:

$$\Delta K = K_{\max} - K_{\min} = \left(\sigma_{\max} - \sigma_{\min}\right)\sqrt{\pi\beta_p a} \tag{29}$$

and β_p is a correction factor that takes into account the finite dimensions of the cracked body.

Initially, Paris proposed a value $n_p = 4$, considered valid for propagation rates between 10^{-6} and 10^{-1} mm/cycle, regardless of the nature of stress.

It can be noted that the relation (28) implies the propagation of the fatigue crack at any value, however small, fact that does not correspond to reality.

The limitations of this relationship are explained by the fact that it is based on the elastic stress-strain solution that is valid only in the outer area of the limited plastic zone that forms at the tip of the crack.

Takashima (cited in [4]) proposed for the non-alloy steels (eq. 30–31) and low-alloy carbon steel (eq. 32–33) the following types of correlations of these parameters depending on the material yield limit (N/mm^2) and the conventional fracture limit (N/mm^2):

$$n_p = 4.52 - 0.26\cdot\sigma_c \tag{30}$$

$$\lg C_p = 0.0483\cdot\sigma_c - 12.432 \tag{31}$$

$$n_p = 5.19 - 0.297\cdot\sigma_r \tag{32}$$

$$\lg C_p = 0.0556\cdot\sigma_r - 13.726. \tag{33}$$

The measurement unit of the parameter C_p is $\dfrac{\text{mm/cycle}}{\left(\text{MPa}\sqrt{\text{mm}}\right)^{n_p}}$.

Many other researchers have proposed empirical relationships for crack propagation. Few of these can be remembered: Klesnil and Lucas, Schijve, Weibull, Mc Evily, Liu, Donahue etc.

4.3. Crack propagation in the mixed mode loading. Equivalent stress intensity factor

For the specific case of the spur gears, although in the substrate of the gear tooth the stresses are mainly compressive, also tensile stresses can occur, for example at the base of the tooth or as a result of the residual stresses resulting from the thermal treatment applied.

These tensions overlap with those of hertzian contact, resulting in a complex loading system.

As it is known, in this case, the values of the stress intensity factor, mode I, become positive, which makes the crack able to grow by the opening mode of the crack flanks. This result in a mixed mode loading, respectively in the growth of the fatigue cracks.

Several models of multiaxial fatigue and crack growth have been proposed in a mixed mode loading. Of these, critical-based models have a higher popularity due to the increased applicability range.

Through these methods, the multiaxial stress field is reduced to an equivalent uniaxial field, based on the observation that fatigue cracks nucleate along a certain plane of material called "critical plane". This plane coincides with the plane of the maximum tangential stress during the crack initiation and with the maximum normal stress plane during its propagation.

The predominance of the type of crack propagation (by sliding the faces or by opening them) is given by the relationship between the tangential and normal stresses or deformations, the material properties, temperature, etc.

In the mixed mode loading, a modified version of the Paris law can be used, which can be expressed using an equivalent stress intensity factor of the form [21, 22, 28]:

$$\mathrm{d}a/\mathrm{d}N = C\left(\Delta K_{eq}\right)^{n}, \tag{34}$$

in which C and n are material constants.

There are several criteria proposed in the literature for calculating the equivalent stress intensity factor corresponding to modes I and II of propagation, of which one can remember:

– Tanaka model [22] – it provides a good correlation with the experimental results:

$$\Delta K_{eq} = \left(\Delta K_I^4 + 8\Delta K_{II}^4\right)^{\frac{1}{4}}. \tag{35}$$

– Yan model [28] is an equation obtained by extending the maximum tangential stress criterion to the mixed mode loading:

$$\Delta K_{eq} = \frac{1}{2}\cos\frac{\theta}{2}\cdot\left[\Delta K_I\left(1+\cos\theta\right)-3\Delta K_{II}\sin\theta\right]. \tag{36}$$

– Richard model [21] – the proposed empirical model is:

$$K_{eq} = \frac{1}{2}\left[K_I + \sqrt{K_I^2 + 4\left(\varsigma_C \cdot K_{II}\right)^2}\right]. \tag{37}$$

4.4. Crack growth initiation angle

The crack propagation trajectory can not be determined unless the angle at which the growth of the crack is known.

The most common criteria can be synthetized into three groups: stress-based criteria, energy criteria, and deformation criteria, respectively. Of these, the most commonly used are those based on tensions as well as energy ones.

Polar expression of the state of tensions at the crack tip is used (Fig. 7).

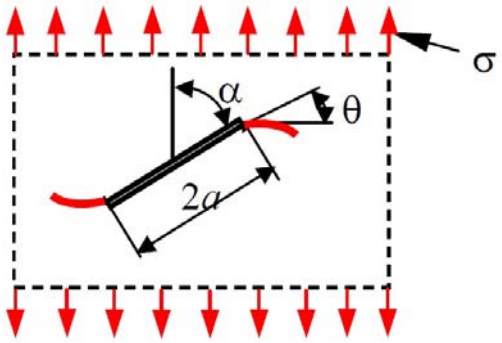

Fig. 7 – Crack growth initiation angle.

– M Criterion. This criterion is also called the maximum triaxial stress criterion and was presented by Kong and others [11]. It considers that the direction of increase of the initial crack coincides with the direction of the maximum triaxial tension along a constant radius around the crack tip. M criterion can be expressed by the relationship of form:

$$\frac{\partial M}{\partial\theta} = 0\,, \quad \frac{\partial^2 M}{\partial\theta^2} < 0\,. \tag{38}$$

Triaxial tension is defined as the ratio:

$$M = \sigma_H / \sigma_{eq} \,, \tag{39}$$

where: σ_H – hydrostatic stress related to plane deformation conditions;
σ_{eq} – the von Mises equivalent stress for plane deformation at the crack tip.

The expressions of these tensions are [10]:

$$\sigma_H = \frac{\sigma_x + \sigma_y + \sigma_z}{3} = \frac{2(1+\nu)}{3\sqrt{2\pi r_a}} \cdot \left(K_I \cos\frac{\theta}{2} - K_{II} \sin\frac{\theta}{2} \right) \tag{40}$$

$$\sigma_{eq} = \left[\frac{(\sigma_x - \sigma_y)^2 + (\sigma_y - \sigma_z)^2 + (\sigma_z - \sigma_x)^2 + 6\tau_{xy}^2}{2} \right]^{\frac{1}{2}} \tag{41}$$

$$\sigma_{eq} = \frac{1}{\sqrt{2}\sqrt{2\pi r_a}} \cdot \left\{ \left(\frac{3}{2} K_I^2 - \frac{9}{2} K_{II}^2 \right) \sin^2\theta + \left[2(1-2\nu) K_I^2 + 6 K_{II}^2 \right] \cos^2\frac{\theta}{2} + \right.$$
$$\left. + 8\left(1 - \nu - \nu^2\right) K_{II}^2 \sin^2\frac{\theta}{2} + K_I K_{II} \left[3\sin 2\theta - 2(1-2\nu)^2 \sin\theta \right] \right\}^{\frac{1}{2}} \tag{42}$$

– **T CRITERION**. This criterion was proposed by Theocaris [25, 26]; he postulates that the direction of the crack growth coincides with the direction of the maximum deformation energy along a contour around the crack tip, where the deformation energy is constant.

To define the region near the crack tip, this criterion uses the elastoplastic boundary conditions.

The mathematical form of this criterion can be expressed in relations as:

$$\frac{\partial T_V}{\partial \theta} = 0 \,, \quad \frac{\partial^2 T_V}{\partial \theta^2} < 0 \tag{43}$$

in which T_V is the energy of deformation and is defined by the relation:

$$T_V = \frac{1-2\nu}{6E} \left(\sigma_x + \sigma_y \right)^2 \tag{44}$$

Other criteria may also be mentioned, such as: S criterion (of the deformation energy density factor), I_p criterion etc.

5. CONCLUSIONS

This article briefly presented the importance of the fatigue cracks which are formed in the substrate of the spur gear teeth, resulting in the appearance of pitting wear.

The main stages of fatigue cracking were presented. There were analyzed the stage of the initiation of the fatigue crack, then the growth of a small crack in the macroscopic crack, and finally, the long-range propagation.

The crack initiation stage can be divided in two parts, namely: crack initiation and small crack growth. The Tanaka-Mura model of crack initiation was briefly presented. Then, few considerations about the growth of a nucleated fatigue crack were highlighted.

An important section of the article corresponds to the presentation of the mechanisms that govern the crack propagation process. The stress field near the crack tip was presented, and also de significance of the stress intensity factor, correlated with the three modes of materials fracture.

It has been shown how the crack growth rate can be determined, the crack propagation in the mixed mode loading and also the equivalent stress intensity factor.

Finally, few criteria concerning the crack growth initiation angle were presented.

All these elements should be considered when studying the cracks occurring in the spur gears, resulting in appearance of the pitting wear.

Received on June 19, 2017

REFERENCES

1. BILBY, B. A., ESHELBY, J. D., *Dislocations and the theory of fracture*, Fracture, **1**, pp. 99–182, 1968.
2. BROEK, D., *Elementary engineering fracture mechanics*, Martinus Nijhoff Publishers, Hague,1984.
3. CHAN, K.S., LANKFORD, J., *A crack tip strain model for the growth of small fatigue cracks*, Scripta Metall., **17**, *4*, pp. 529–532, 1983.
4. CIOCLOV, D., *Fracture Mechanics* (in Romanian), Editura Academiei R.S.R., Bucharest, 1977.
5. CIZELJ, L., SIMONOVSKI, I., *Multiscale modeling of short cracks in random polycrystalline aggregates*, Materials and Technology, **41**, *5*, pp. 227–230, 2007.
6. COLAGELO, V.J., HEISER, F.A., *Analysis of metallurgical failures*, 2nd Edition, John Wiley and Sons, Inc., 1987.
7. DAVIDSON, D.L., *Characterizing small fatigue cracks in metallic alloys*, Metall. and Mat. Transactions A, **35**, *1*, pp. 7–14, 2004.
8. GDOUTOS, E.E., *Fracture mechanics. An introduction*, 2nd Edition, Springer, Dordrecht, 2005.
9. IRWIN, G. R., *Analysis of stresses and strains near the end of a crack traversing a plate*, ASME J. of Applied Mechanics, **24**, *3*, pp. 361–364, 1957.
10. KHAN, S.M.A., KRAISHEH, M.K., *Analysis of mixed mode crack initiation angles under various loading conditions*, Engineering Fracture Mechanics, **67**, *5*, pp. 397–419, 2000.
11. KONG, X.M., SCHLUTER, N., DAHL, W., *Effect of triaxial stress on mixed-mode fracture*, Eng. Fracture Mech., **52**, *2*, pp. 379–388, 1995.
12. KUDISH, I.I., *A New Statistical Model of Contact Fatigue*, Tribology Transactions, **43**, *4*, pp. 711–721, 2000.

13. MC DOWELL, D.L., BENNETT, V.P., *A microcrack growth law for multiaxial fatigue*, Fatigue & Fracture of Engineering Materials & Structures, **19**, *7*, pp. 821–837, 2007.
14. MOUSA, J.H., *Experimental and numerical analyses of mixed mode crack initiation angle*, PhD Thesis, King Fahd University of Petroleum & Minerals, Dhahran, Saudi Arabia, 2006.
15. MURAKAMI, Y., *Metal fatigue: effects of small defects and nonmetallic inclusions*, Elsevier Science Ltd., Oxford, 2002.
16. MURAKAMI, Y., *Stress intensity factor handbook*, Vols. I and II, Pergamon Press, 1987.
17. MUSKHELISHVILI, N.I., *Singular integral equations*, Noordoff Inter., 1977.
18. PARIS, P.C., GOMEZ, M., ANDERSSON, E.E., *A rational analytic theory of fatigue*, The Trend in Engineering, **13**, *1*, pp. 9–14, 1961.
19. PINAU, A., *Short fatigue crack behavior in relationship to three-dimensional aspects and crack closure effect*, in: *Small fatigue cracks* (Eds. R.O. Ritchie and J. Lankford), The Metallurgical Society, Warrendale, 1986, pp. 213–223.
20. POPA, C.O., *Modern state in modeling rolling contact fatigue phenomenon*, The 1st International Conference: *Advanced Engineering in Mechanical Systems* (ADEMS'07), Acta Technica Napocensis, Series: Applied Mathematics and Mechanics, **50**, *2*, pp. 401–408, 2007.
21. RICHARD, H.A., *Role of fracture mechanics in modern technology*, Elsevier Science Publishing, North-Holland, 1987.
22. TANAKA, K., *Fatigue crack propagation from a crack inclined to the cyclic tensile axis*, Engng. Fracture Mech., **6**, *3*, pp. 493–507, 1974.
23. TANAKA, K., MURA, T., *A dislocation model for fatigue crack initiation*, ASME J., Appl. Mech., **48**, *1*, pp. 97–103, 1981.
24. TANAKA, K., KINEFUCHI, M., YOKOMAKU, T., *Modeling of statistical characteristics of the propagation of small fatigue cracks*, in: *Short fatigue cracks* (Eds. K.J. Miller and E.R. de los Rios), ESIS 13, pp. 351–368, Mechanical Engineering Publications, London, 1992.
25. THEOCARIS, P.S., KARDOMATEAS G.A., ADRIANOPOULOS N.P., *Experimental study of T-criterion in ductile fracture*, Eng. Fracture Mech., **17**, *5*, pp. 439–447, 1982.
26. THEOCARIS, P.S., ADRIANOPOULOS N.P., *The T-criterion applied to ductile fracture*, Int. J. of Fracture, **20**, *4*, pp. 125–130, 1982.
27. TYRON, R.G., *Probabilistic mesomechanical fatigue model*, NASA Contractor Report 202342, Grant NGT-51053, Lewis Research Center, 1997.
28. YAN, X., ZHANG, Z., DU, S., *Mixed mode fracture criteria for materials with different yield strengths in tension and compression*, Engng. Fracture Mech., **42**, *1*, pp. 109–116, 1992.